Experimental Study and Model for Healthy and Pathological Synovial Fluid

Thomas B. GOUDOULAS *, Eleftherios G. KASTRINAKIS

* Corresponding author: Tel.: ++30 2310996239; Fax: ++30 2310996190; Email: thomas@eng.auth.gr
School of Engineering, Chemical Engineering Department, Aristotle University of Thessaloniki, GR

Abstract In the present work a comparative rheological study of healthy and pathological synovial fluid (SF) is presented. The SF samples were obtained from healthy dogs or dogs with rupture of cranial cruciate ligament. The rheological measurements were carried out at 25 ^{o}C and 38 ^{o}C, i.e. at room temperature and at the regular temperature of the dog's body. A stainless steel rotating disk of 20 mm diameter was used on the rheometer AR-G2 and the gap between the plate and the disk was up to 125 μm. It was found that for the healthy SF, the viscosity was reduced by three orders of magnitude (from 40 Pa·s to 0.04 Pa·s) as $\dot{\gamma}$ was increased from 10^{-3} up to 800 s^{-1}. For the pathological cases and for the same range of shear rates the viscosity values were between 1 Pa·s and 10^{-2} Pa·s. An established rheological model, i.e. the Carreau model, was used to describe the flow curves with successful results. Finally, the viscoelastic behavior was recorded by oscillatory and creep measurements and the obtained results indicate that the retardation time increases in consecutive measurements and also that the Cox-Merz rule is applicable in SF rheology.

Keywords: Synovial Fluid, Hyaluronan, Glycosaminoglycan, Viscoelastic Behavior, Shear-thinning Fluid

1. Introduction

The joints of the limbs of primates are unique creations in terms of engineering and operational structure. In a joint, the fluid component that provides lubricating action and prevents the direct contact of the cartilage surfaces is called synovial fluid (SF). The SF is a derivative of blood serum via a natural process of osmosis in joint cavity. It has the one third of the proteins concentration of blood and contains only the proteins of small molecular weight, such as albumin (Jay et al. 2007). The main component of SF, however, is the linear, high molar mass, non-sulfated glycosaminoglycan, i.e. the Hyaluronic Acid (HA). The HA is considered as the controlling parameter for an effective function of healthy SF in joints (Lee and Spencer 2008; Kogan et al. 2007, Schurz 1996). The unique structures of HA and proteoglycans in SF, are fundamentals for SF function as an indisputable successful biolubricant in all primates; the rearrangement of such structures gives a shear-thinning behavior of SF along with remarkable viscoelastic behavior (Gomez and Thurston 1993; Kogan et al. 2007). For instance, it has been reported (Hussainova and Ghaemi 2008; Jay et al. 2007) that HA and lubricin synergistically decrease the friction at the cartilage-cartilage interface by some sort of selective adhesion. Yet, the influence of proteins on the SF rheology and the interaction with HA is still under consideration (Bingöl et al. 2010).

The condition of the joint, i.e. healthy or pathological, affects the mean molecular weight of the HA, which ranges from the order of magnitude of 10^5 up to 10^6 Da (Schurz 1996). Along with the mean molecular weight of HA its concentration is also affected, so it could be from 1.5 up to 3.5 mg HA per ml SF, for the lower to the highest reported concentration, respectively (Fam et al. 2007). Therefore, it is obvious that the SF rheology can control the tribology of the joints either of healthy people, or of individuals with pathological problems (Davies and Palfrey 1968, Schurz 1996). For instance, altered rheological behavior has been reported (Barbucci et al. 2002; Fam et al. 2007) at the appearance of arthritis or osteoarthritis and the reduced viscoelastic properties have been used as an undeniable evidence of this change (Fam

et al. 2007; Gomez and Thurston 1993).

In the present paper, experimental rheological data of healthy and pathological SF obtained from adult dogs, along with an application of a rheological model on obtained experimental data, are reported in order to provide means for simulation of the SF rheology in micro flows.

2. Materials and Methods

2.1 Healthy and pathological SF samples

The SF samples were obtained with arthrocentisis under aseptic conditions, from the knee joint of adult dogs (weight > 20 Kg). The pathological SF samples were from clinical cases of dogs with rupture of cranial cruciate ligament. The healthy ones were from clinical cases irrelevant to orthopaedic injuries. 21G needles attached to 2.5 or 5 ml syringes were used to obtain the SF samples. In most cases volumes of 1 to 1.5 ml were aspirated. During the procedure all animals were under sedation or general anaesthesia; the protocol of acquiring the SF samples was approved by the Ethical Committee of the Companion Animal Clinic of the Veterinary School of the Aristotle University of Thessaloniki (AUTh). In addition, informed consent from the owners was obtained in all cases. When storage of samples was inevitable, the SF samples were stored in aliquots at –24 ^{o}C until analyzed.

2.2 Rheological measurements

The measurements of the present work were carried out with the rheometer AR-G2 (TA Instruments) using parallel disks geometry, having a stainless steel rotating disk of 20 mm diameter while the gap was up to 125 μm, mainly due to the small quantities of the SF samples. Certified standard oils were used regularly for calibration of the rheometer. The measurements were carried out at two temperatures of 25 ^{o}C and 38 ^{o}C, i.e. at ambient temperature and at regular animal's body temperature. The accuracy of the applied temperature was ±0.1 ^{o}C by the Peltier system of the rheometer which was also the plate where the SF samples were placed. Finally, a cylindrical Plexiglas cover was used to cover the rotating geometry and the SF sample (under the geometry), providing a closed volume. This volume was effectively saturated with water via the wetted material at its periphery.

After the aspiration procedure, no preshear conditions were applied prior to the measurements, in order to evaluate the rheological behavior of SF as being at rest, and the data hereinafter refer to non-preshear conditions. In this way, the sample loading on the rheometer was performed without using needles. Shear flow measurements were performed to get the flow curves of the various SF samples, i.e. viscosity η (Pa·s) measurements at various shear rates $\dot{\gamma}$ (s^{-1}). The achieved shear rates were between 10^{-4} s^{-1} and 10^{3} s^{-1}.

To attain a complete rheological characterization of the SF samples, measurements of the storage and loss modulus G′ and G′′ (Pa), respectively, were performed for various applied frequencies and strains. Additional parameters of the viscoelastic behavior, like the complex viscosity η^* and the dynamic viscosity η' (Pa·s) were also calculated by the software of the rheometer. To determine the linear viscoelastic region of the SF samples small amplitude oscillatory measurements were performed. The criteria were the in-phase non-distorted and reproducible waveforms, both in applied and in measured strain. In the strain sweep tests, the strain amplitude γ% was varied from 0.1 to 50 %, at a fixed oscillation frequency (3.14 rad·s^{-1}), and it was found that the linear viscoelastic region was extended up to 5% strain amplitude. In the frequency sweep measurements, the angular frequency ω (rad·s^{-1}) was varied from 0.1 to 30 rad·s^{-1}, corresponding to a frequency range from 0.015 Hz up to 5 Hz, approximately. The applied frequencies cover the walking and running frequencies, i.e. 0.2-0.5 Hz and 1.5-2 Hz, respectively.

Creep measurements, which provide additional information about the viscoelastic behavior and the steady state viscosity at low shear rates (the "zero shear viscosity" η_0), were also performed on SF samples. In creep

experiments the applied shear stress σ (Pa) must be sufficiently small, so the produced time-dependent shear strain, γ(t), will remain within the linear region. In this case, the characteristic material function is the creep compliance $J(t)$ (Pa^{-1}), which is defined as the ratio of $\gamma(t)$ over σ. At long enough time, the shear rate $\dot{\gamma}$ approaches a steady value and the linear asymptote to the creep curve is the η_0 viscosity.

3. Results and Discussion

The experimental data show that the healthy SF exhibits non-Newtonian shear thinning behavior over five orders of magnitude of shear rate. The achieved shear rate values in the low shear region, by using the AR-G2 rheometer, were of the order of magnitude of 10^{-3} s^{-1} and the viscosity values of about 40 Pa·s, for 25 ^{o}C temperature.

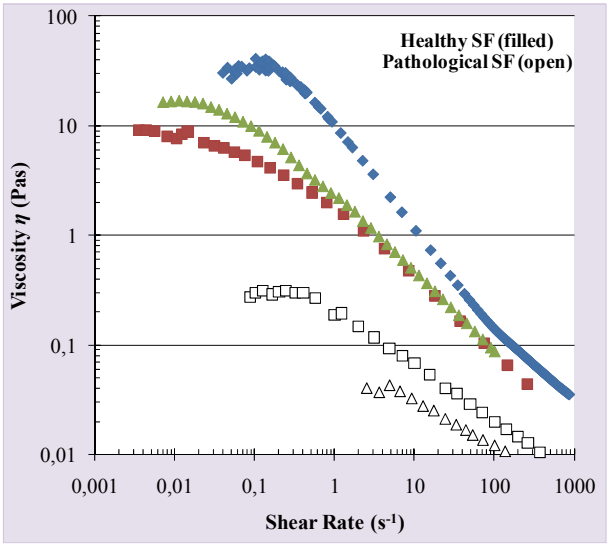

Fig. 1. Healthy (filled symbols) and pathological (open symbols) SF flow curves for 25 ^{o}C. Each curve corresponds to a different animal.

The same behavior qualitatively was observed for higher temperatures, e.g. 38 ^{o}C (not shown here) in accordance with previous work (Goudoulas et al. 2010). From Fig.1 it can be seen that for the same shear rate value (e.g. 10 s^{-1}) the healthy SF samples exhibit an order of magnitude higher viscosity than the pathological ones. The upper Newtonian plateau was also present in all cases studied, i.e. the zero shear viscosity η_0. Based on this observation a model fitting was attempted with models including the η_0 parameter, i.e. Williamson, Cross, Ellis, and Carreau rheological models. It must be pointed out that the selection of the appropriate model was based on the minimum standard error of the fitting. The Carreau model fits on the data of Fig. 1 with the minimum standard error and is written as follow:

$$\frac{\eta-\eta_\infty}{\eta_0-\eta_\infty}=\frac{1}{\left(1+(c\dot{\gamma})^2\right)^{b/2}} \qquad (1)$$

where, η_0, η_∞, are the zero and infinitive shear viscosity, respectively, while the parameters c and b are the consistency and shear rate index, respectively. Finally, the results of the fitting are presented in Fig. 2. It is noticeable that in the studied shear rate range (10^{-3} s^{-1} to 10^{3} s^{-1}) the high shear Newtonian plateau is not present. Possibly $\dot{\gamma}$ values of the order of 10^{4} s^{-1} will result in the η_∞.

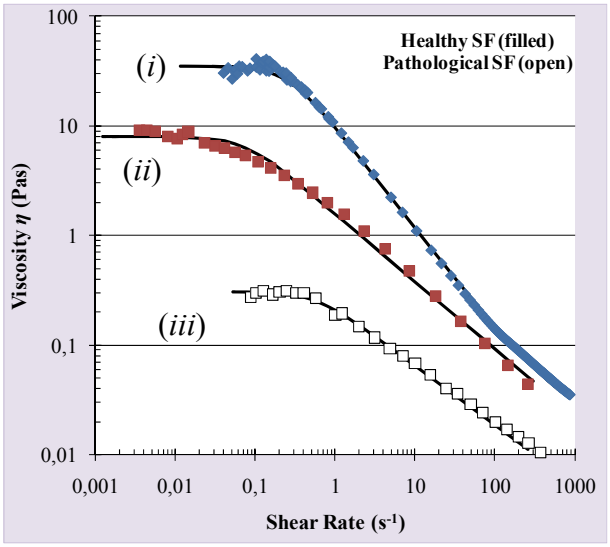

Fig. 2. Selected data of Fig.1 along with fitting curves of Carreau model (solid black lines).

Detailed values of the fitting for the flow curves of Fig. 2 are presented in the following Table 1, along with results of Williamson model for comparison reasons.

Table 1. Detailed values of fitting in Fig. 2.

Model	η_0 / Pa·s	consistency, c / sec	rate index, b/-
Carreau			
Curve *i*	31.5	3.92	0.935
ii	7.93	14.12	0.615
iii	0.304	1.76	0.538
Williamson			
Curve *i*	37.2	2.75	0,962
ii	9.58	8.95	0.692
iii	0.432	1.59	0.5885

Three consecutive creep measurements are representatively shown in Fig. 3 with applied stress of 4×10^{-3} Pa, on a healthy SF sample at 25 °C.

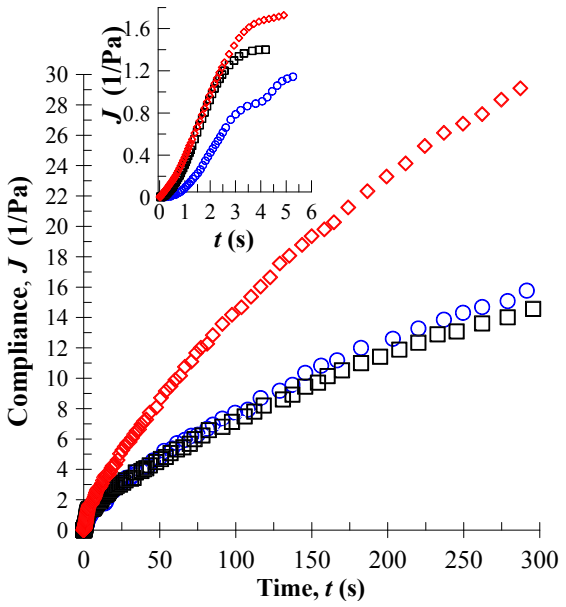

Fig. 3. Creep measurements consecutive on the same sample of healthy SF (applied stress = 4×10^{-3} Pa). The order was: ◇ first, ○ second, □ third. (Temp. = 25 °C)

It must be mentioned that the initial value of the compliance $J(t)$, i.e. the J_0, corresponds to purely elastic response of the material. This value is recorded during the first few seconds of the creep measurement (inset plot for details). By plotting data in logarithmic scale (not shown here) it was found that the J_0 is small, of the order of magnitude of 10^{-4}. Next is presented a fit of a discrete retardation model on experimental measurement of SF.

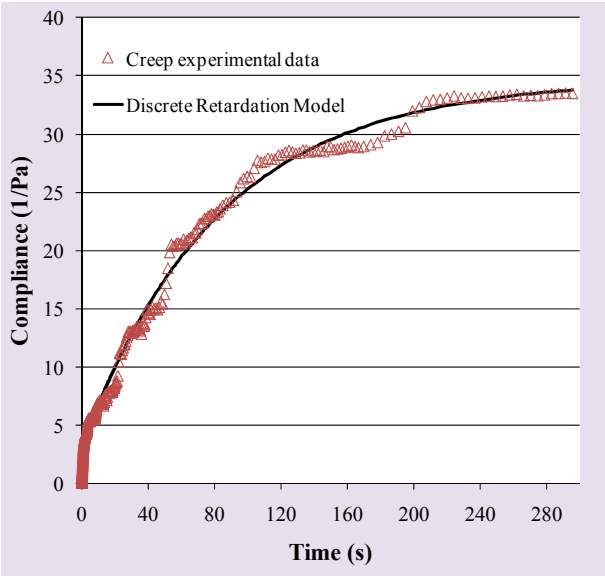

Fig. 4. Creep measurement of a healthy SF sample, with applied shear stress 0.64×10^{-3} Pa. (Temp. = 25 °C)

The general equation of the creep compliance is the following one:

$$J(t) = J_0 + \sum_{i=1,2,3\ldots} J_i(1-\exp(-t/t_{Ri})) + t/\eta_0 \quad (2)$$

The three parameters in the right-hand side of Eq. 2 are the elastic response J_0, as described previously, the viscoelastic response, represented by the sum of the *i*-elements, and finally the asymptotic Newtonian behavior (i.e., creep viscous flow where the $J(t)$ is linear with time t). The parameters J_i and t_{Ri} are the compliance and the characteristic retardation time of each element. For long enough time of measurement, each element is equal to J_i and the sum in Eq. 2 is practically equal to $\sum_{i=1,2,3\ldots} J_i$.

Thus, is easy to find the 'zero shear viscosity' η_0, that is $t/[J(t) - J_0 - J_1 - J_2 - J_3\ldots]$. Therefore, data in Fig. 3 indicate that the η_0 of the SF sample increases from the first measurement to the second.

Analysis of the data in Fig. 4 by the software of the rheometer AR-G2 (Rheology Advantage Data Analysis, V5.7.1, TA

Instruments) gives the discrete retardation spectrum of this creep measurement. It consists of six elements with the longest retardation time, t_{Ri}, equal to 81.6 s while the smallest was 4.6×10^{-3} s. Also, the zero shear viscosity η_0 was 1174 Pa·s corresponding to steady state shear rates of the order of magnitude of 10^{-4} s^{-1}, while the J_0 compliance was 4.46×10^{-6} 1/Pa. Hence, the product $\eta_0 J_0$ gives a "characteristic overall" retardation time equal to 5.7×10^{-3} s. This result is in accordance with previous reported work (Goudoulas et al. 2010).

The six elements of the discrete retardation spectrum, required to describe the creep experiment, indicate that the macromolecules do not have one single molecular weight. It is possible that a distribution of molecular weights exists and each element represents the behavior of an individual biopolymer fraction. Along with the observations of Fig. 3, the results of the discrete retardation analysis in Fig. 4 indicate that the SF manly behaves as a viscoelastic fluid rather than an elastic material.

Oscillatory measurements were carried out to reveal the linear viscoelastic behavior of the SF. Typical results of mechanical spectra, for a healthy SF sample at 38 °C, are presented in Fig. 5.

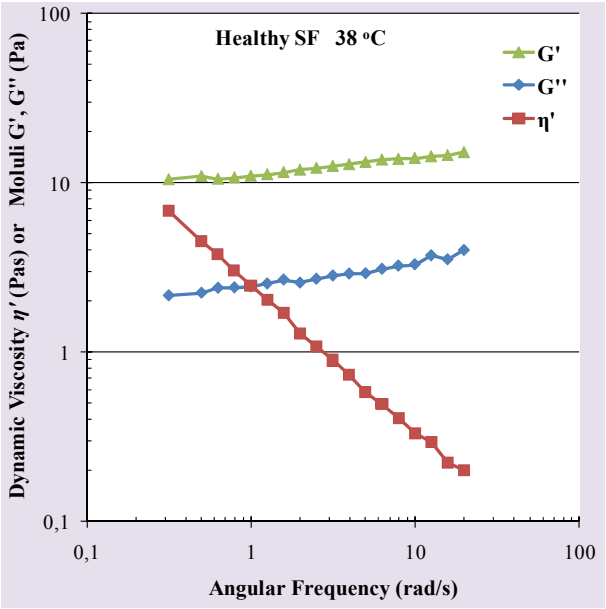

Fig. 5. Results of frequency sweep (strain 1%) at 38 °C. Healthy SF sample.

The recorder behavior is typical behavior of dense solutions of entangled macromolecules, i.e. the G´ about an order of magnitude higher than the G´´ and the dynamic viscosity η' smoothly decreases almost two orders of magnitude over the applied frequency range. By analyzing such measurements of linear viscoelastic behavior, it is apparent that the macromolecules of HA overlapping each other and interacting through physical entanglements, possibly supported by the small molecular weight proteins (lubricin, albumin) (Jay et al. 2007).

Considering dynamic data (similar of those in Fig. 5) and re-plotted together with the steady state shear data (similar to those in Fig. 1) in the same plot, the relationship between the linear (oscillatory) and the non-linear viscoelastic properties (flow) becomes evident. The results are summarized in Fig. 6.

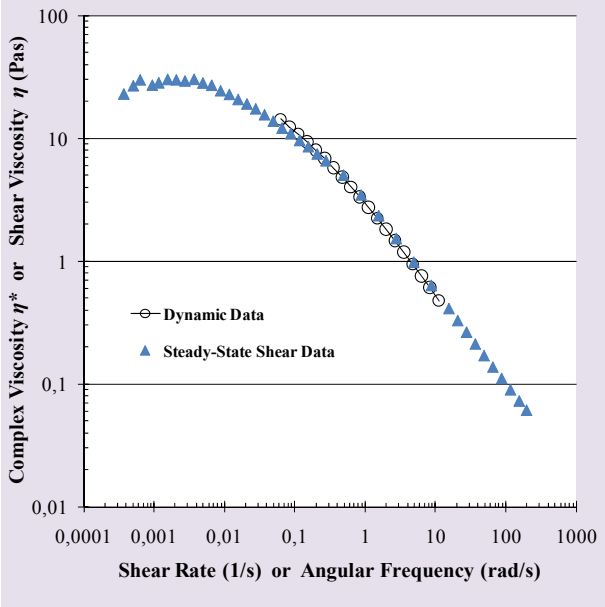

Fig. 6. Complex viscosity $|\eta^*|$ as a function of applied frequency ω and steady state shear viscosity $\eta(\dot{\gamma})$ as a function of shear rate. (Temp. = 25 °C)

Data in previous Fig. 6 correspond to the same SF sample, either in oscillatory or in flow experiments. It is observed that the steady state shear viscosity $\eta(\dot{\gamma})$ coincide with the magnitude of the complex viscosity $|\eta^*|(\omega)$.

This condition is known as the empirical Cox-Merz rule. Such good agreement is often obtained for solutions of entangled macromolecules, while deviations are reported in cases of cross-linked structure formations, where $|\eta^*|(\omega)$ is in general larger than the steady-state shear viscosity (Winter 2009). These results are very encouraging since, in general, small quantities of SF are available so the number of measurements is limited and the results indicate that either the dynamic or the steady shear data are practically the same.

4. Conclusions

By considering the Carreau rheological model as a representative one of the steady-state values of shear viscosity, a model fitting of the healthy and pathological SF shear rheology could be achieved. Moreover, characteristic times of entanglements of HA in the molecular network of SF were recorded via creep measurements. Given that HA shows little intermolecular association, the structural organization of SF would be determined by the ratio of the characteristic time to the inverse of the shear rate, e.g. if the strain is small enough, the induced changes in the structure are slower than the time scale determined by the inverse of the shear rate. Finally it was shown that the Cox-Merz rule is applicable in SF rheology signifying that the SF structure under shear conditions is similar to those solutions of linear and entangled macromolecules.

5. Acknowledgments

The authors are indebted and thankful to Associate Prof. L. Papazoglou, Assistant Prof. G. Kazako, and PhD candidate P. Kosma from Companion Animal Clinic of the Veterinary School of AUTh for providing systematically the SF samples.

6. References

Barbucci, R., Lamponi, S., Borzacchiello, A., Ambrosio, L., Fini, M., Torricelli, P. and Giardino, R., 2002. Hyaluronic acid hydrogel in the treatment of osteoarthritis. Biomat. 23, 4503–4513.

Bingöl, A.Ö., Lohmann, D.K., Püschel, K. and Kulicke, W.-M., 2010. Characterization and comparison of shear and extensional flow of sodium hyaluronate and human synovial fluid. Biorheol. 47, 205–224.

Davies, D.V. and Palfrey, A.J., 1968. Some of the physical properties of normal and pathological synovial fluids. J. Biomech. 1, 79–88.

Fam, H., Bryant, J.T. and Kontopoulou, M., 2007. Rheological properties of synovial fluids. Biorheol. 44(1-2), 59–74.

Gomez, J.E. and Thurston, G.B., 1993. Comparisons of the oscillatory shear viscoelasticity and composition of pathological synovial fluids. Biorheol. 31(5-6), 409–427.

Goudoulas, T.B., Kastrinakis, E.G., Nychas, S.G., Papazoglou, L.G., Kazakos, G.M., Kosmas, P.V., 2010. Rheological study of synovial fluid obtained from dogs: Healthy, pathological, and post-surgery, after spontaneous rupture of cranial cruciate ligament. Ann. Biomed. Eng. 38 (1), 57–65.

Winter, H.H., 2009. Three views of viscoelasticity for Cox–Merz materials. Rheol. Acta 48, 241–243.

Hussainova, I. and Ghaemi, H., 2008. Biobearings: where mechanics meets biology. Proc. Estonian Academy of Sciences, 57(4), 232–240.

Jay, G.D., Torres, J.R., Warman, M.L., Laderer, M.C. and Breuer, K.S., 2007. The role of lubricin in the mechanical behavior of synovial fluid. P. Natl. Acad. Sci. USA 104(15):6194–6199.

Kogan, G., Soltes, L., Stern, R., Gemeiner, P., 2007. Hyaluronic acid: a natural biopolymer with a broad range of biomedical and industrial applications, Biotechnol. Lett. 29, 17–25.

Lee, S., and Spencer, N.D., 2008. Sweet, hairy, soft, and slippery. Science 319(5863), 575–576.

Schurz, J. 1996. Rheology of synovial fluids and substitute polymers. J. Macromol. Sci. A 33(9), 1249–1262.